

This is a repository copy of *Long-term prediction of the effects of climate change on indoor climate and air quality*.

White Rose Research Online URL for this paper:

<https://eprints.whiterose.ac.uk/id/eprint/206313/>

Version: Published Version

---

**Article:**

Shaw, David [orcid.org/0000-0001-5542-0334](https://orcid.org/0000-0001-5542-0334) and Carslaw, Nicola [orcid.org/0000-0002-5290-4779](https://orcid.org/0000-0002-5290-4779) (2023) Long-term prediction of the effects of climate change on indoor climate and air quality. *Environmental Research*. 117804. ISSN 0013-9351

<https://doi.org/10.1016/j.envres.2023.117804>

---

**Reuse**

This article is distributed under the terms of the Creative Commons Attribution-NonCommercial-NoDerivs (CC BY-NC-ND) licence. This licence only allows you to download this work and share it with others as long as you credit the authors, but you can't change the article in any way or use it commercially. More information and the full terms of the licence here: <https://creativecommons.org/licenses/>

**Takedown**

If you consider content in White Rose Research Online to be in breach of UK law, please notify us by emailing [eprints@whiterose.ac.uk](mailto:eprints@whiterose.ac.uk) including the URL of the record and the reason for the withdrawal request.



# Long-term prediction of the effects of climate change on indoor climate and air quality

Jiangyue Zhao<sup>a</sup>, Erik Uhde<sup>a</sup>, Tunga Salthammer<sup>a</sup>, Florian Antretter<sup>b,c</sup>, David Shaw<sup>d</sup>, Nicola Carslaw<sup>d</sup>, Alexandra Schieweck<sup>a,\*</sup>

<sup>a</sup> Fraunhofer WKI, Department of Material Analysis and Indoor Chemistry, Riedenkamp 3, 38108, Braunschweig, Germany

<sup>b</sup> C3RRolutions GmbH, Steinbrucker Str. 11, 83064, Raubling, Germany

<sup>c</sup> Fraunhofer IBP, Fraunhoferstraße 10, 83626, Valley, Germany

<sup>d</sup> University of York, Department of Environment and Geography, Heslington, York, YO10 5NG, UK

## ARTICLE INFO

### Keywords:

Thermal discomfort  
Mold growth  
Building physics  
Air pollutants  
Mitigation measures

## ABSTRACT

Limiting the negative impact of climate change on nature and humans is one of the most pressing issues of the 21st century. Meanwhile, people in modern society spend most of the day indoors. It is therefore surprising that comparatively little attention has been paid to indoor human exposure in relation to climate change. Heat action plans have now been designed in many regions to protect people from thermal stress in their private homes and in public buildings. However, in order to be able to plan effectively for the future, reliable information is required about the long-term effects of climate change on indoor air quality and climate.

The Indoor Air Quality Climate Change (IAQCC) model is an expedient tool for estimating the influence of climate change on indoor air quality. The model follows a holistic approach in which building physics, emissions, chemical reactions, mold growth and exposure are combined with the fundamental parameters of temperature and humidity. The features of the model have already been presented in an earlier publication, and it is now used for the expected climatic conditions in Central Europe, taking into account various shared socioeconomic pathway (SSP) scenarios up to the year 2100.

For the test house examined in this study, the concentrations of pollutants in the indoor air will continue to rise. At the same time, the risk of mold growth also increases (the mold index rose from 0 to 4 in the worst case for very sensitive material). The biggest problem, however, is protection against heat and humidity. Massive structural improvements are needed here, including insulation, ventilation, and direct sun protection. Otherwise, the occupants will be exposed to increasing thermal discomfort, which can also lead to severe heat stress indoors.

## 1. Introduction

Today, serious discussions about global climate change involve assessing possible impacts and how to effectively counteract them. It is no longer a question of whether climate change will happen, we are already in the midst of it. The goal of a maximum global warming of 1.5 °C by 2100, which is often declared as a target by politicians, is at the lower end of the actual “very likely range” forecast by the Intergovernmental Panel on Climate Change (IPCC, 2021) and is looking increasingly challenging to achieve. It is therefore advisable to also consider the possibility of more pessimistic scenarios.

Valid predictions regarding future indoor and outdoor climates were published years ago (Brasseur et al., 2017; Fisk, 2015; Jacob and

Winner, 2009; Nazaroff, 2013; Vardoulakis et al., 2015) and independently of the IPCC reports. There are numerous examples of the consequences of extreme weather events (Fischer et al., 2004; Hamdy et al., 2017; Schär and Jendritzky, 2004; Steul et al., 2018), as well as calculations of indoor and outdoor air pollutant concentrations (Lacressonnière et al., 2017; Lee et al., 2006; Salthammer et al., 2018; Zhong et al., 2017) cited and discussed in these publications.

Various organizations have drawn up action plans to protect human health from extreme heat. The World Health Organization (WHO) published guidance on heat-health action in 2008, which was updated in 2021 (World Health Organization, 2021a). In Germany, the working group “Health Adaptation to the Consequences of Climate Change” has developed recommendations for heat action plans to protect human

\* Corresponding author.

E-mail address: [alexandra.schieweck@wki.fraunhofer.de](mailto:alexandra.schieweck@wki.fraunhofer.de) (A. Schieweck).

<https://doi.org/10.1016/j.envres.2023.117804>

Received 6 October 2023; Received in revised form 15 November 2023; Accepted 26 November 2023

Available online 30 November 2023

0013-9351/© 2023 The Authors. Published by Elsevier Inc. This is an open access article under the CC BY-NC-ND license (<http://creativecommons.org/licenses/by-nc-nd/4.0/>).

health. A report commissioned by the German Environment Agency (Umweltbundesamt – UBA) assesses the risk for the indoor climate by the end of the century without adaptation as medium to high (Bund/Länder Ad-hoc Arbeitsgruppe Gesundheitliche Anpassung an die Folgen des Klimawandels, 2017; Kahlenborn et al., 2021). The available action plans are a step in the right direction. However, the information chain from planning to implementation often requires complex logistics, which take time and considerable challenges. Ultimately, it is local authorities who must implement the appropriate measures.

In addition, most of the available recommendations only refer to the temperature, but the human heat balance is also dependent on the air humidity. With increasing humidity, it becomes more difficult to cool the body by evaporation of sweated water (McArdle et al., 2014). Consequently, the so-called heat stress indices always take both parameters into account (Salthammer and Morrison, 2022).

As shown in Fig. 1, there are many other climate change related events that will affect the indoor environment. This includes extreme cold, the risk of mold formation under high humidity, the formation of photo smog, in particular tropospheric ozone and OH radicals through UV radiation as well as other air pollutants such as NO<sub>x</sub>, particles and organic compounds. In order to be better prepared for short- and long-term climate events with regard to the living environment, valid predictions and recommendations are therefore necessary. In the short term, residents need to know how to protect themselves against extreme heat, moisture and air pollutants. If necessary, decisions have to be made on a daily basis, e.g. whether it is better to stay at home, or how and at what time of day the living space should be ventilated. In the medium term, practical information on the implementation of structural thermal insulation (Fisk et al., 2020), intelligent ventilation and heating systems (Schieweck et al., 2018), as well as protection from mold (Nevalainen et al., 2015) and bioaerosols (Nazaroff, 2016) is required.

Mansouri et al. (2022) state in their review that the influence of climate change on indoor air quality (IAQ) remains largely unknown and the evolution of many influencing factors is unpredictable. It is of course undisputed that the exact consequences of climate change for nature and society are still unknown. However, certain events are very likely to occur or have already occurred, and it is definitely possible to prepare for this. With the Indoor Air Quality Climate Change (IAQCC) model, we recently reported on a holistic tool developed by us, which allows short- and long-term predictions of IAQ (Salthammer et al., 2022). The strength of this tool lies in the fact that it couples a model for pollutant release and transport with a building physics model. The calculations can be performed at different technical levels so that they can

be used by both experts and non-experts.

In this further work, we make predictions for the future development of indoor climate, air quality and mold growth based on our IAQCC model, whereby we consider long-term developments until 2100 as well as short-term extreme situations. To the best of our knowledge, this is the first work to provide long-term projections of the effects of climate change on IAQ and occupant well-being, taking into account the complex impacts of building physics, physical and chemical processes of airborne pollutants. We believe that this provides valuable assistance for a more comprehensive assessment of upcoming climate events and for the more rigorous development of preventive measures.

## 2. Methods

### 2.1. IAQCC model description

The concept of the IAQCC model has been published previously (Salthammer et al., 2022) and is now applied to short- and long-term predictions of IAQ. The IAQCC model was developed to quantify the impact of different future ambient climate and emission scenarios on indoor climate and air quality. It can be used to identify reliable trends by considering building parameters and residential activities. The holistic approach combines five sub-models that individually tackle:

- Building heat and moisture transfer,
- Gaseous and particulate emissions from indoor materials and activities,
- Gaseous chemical reactions and aerosol particle dynamics,
- Mold growth,
- Occupant comfort and pollutant exposure estimation.

Indoor air pollution simulation models (including gas and particle models) were built in as a plug-in function based on WUFI® (Wärme Und Feuchte Instationär, engl. heat and moisture transiency) software.

### 2.2. Test house settings for simulation

In our previous work (Salthammer et al., 2022), temperature and humidity were simulated and validated by measurements for a house in Braunschweig (test house 1) during the 2021 summer period. The test house 1 was operated under strict ventilation rules, i.e. doors and windows were opened in the morning and evening and closed during the day. It was also equipped with shading devices that were used regularly. To emphasize the influence of the climate and reduce the influence of the occupants, for the current work we chose another house (test house 2) with less ventilation control and no shading device. From this point on, the “test house” will always refer to test house 2.

A two-story single-family house located close to Braunschweig (longitude 10.74 E; latitude 52.07 N), Germany, was selected as a test house for simulation. The house is an old building (built around 1850–1870), which was retrofitted in 2016 under the requirement of the German Energy Saving Ordinance (EnEV) applicable at that time. The calculated heat transfer coefficient (U-value) for the outer wall is 0.197 (W/m<sup>2</sup>·K). Three double-glazed windows (1.5 m<sup>2</sup> each) face east. The U-value was assumed to be 2.7 (W/m<sup>2</sup>·K) (Weller et al., 2009). The outer wall even complies with the current status (2023) of the German Building Energy Act (GEG, 2020) regulation for existing buildings, where the required U-value for the outer wall should be below 0.24 W/(m<sup>2</sup>·K). The windows, on the other hand, do not meet the current requirement (U < 1.3 W/(m<sup>2</sup>·K)). Nevertheless, the insulation situation of this house reflects the reality of new construction and retrofitting in Germany.

The simulation zone in the model is the main living room located on the ground floor with a total volume of 85 m<sup>3</sup> (width = 4.9 m, length = 6 m, height = 2.9 m). The room has an estimated furniture area of 135 m<sup>2</sup>, together with the surface area of the walls, ceiling and floor

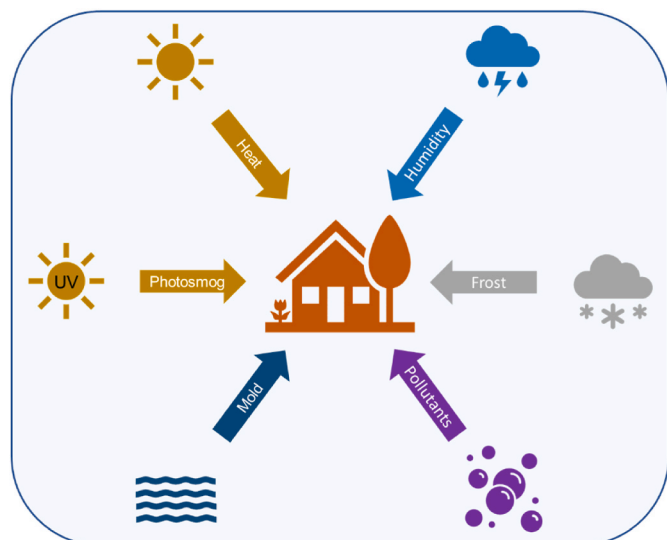


Fig. 1. Parameters associated with climate change affecting indoor air quality.

resulting in an A/V ratio of 3 (m<sup>2</sup> m<sup>-3</sup>), which is typical for furnished homes (Carslaw, 2007; Wainman et al., 2001). The wall heating was switched on during the typical “heating period” in Germany (October–April), and the room air temperature was assumed with a minimum of 16 °C in the model. The simulation room assumes an internal heat and moisture load associated with 2 people sitting quietly.

The test house is manually ventilated. The occupants usually leave the windows tilted (tilt opening from the top, which is common for windows in Germany) during the summer months (June–August), so that the air change rate for this period is 1.5 h<sup>-1</sup>, a value between the open and closed state of the windows (see Section 2.4). For the rest of the year, the occupants do not have a fixed schedule for opening the windows, so a constant air change rate of  $\lambda = 0.5 \text{ h}^{-1}$  was assumed. The simulation results for room temperature and relative humidity were also validated with measured data for one month (see Supporting Information).

### 2.3. Parameters for the building physics model

The building physics model builds on the hygrothermal whole building simulation software WUFI® Plus (Antretter et al., 2015), which is used to calculate energy demand and indoor building climate. It models in detail the building components (walls, floors, ceilings, windows), building usage and inner sources, ventilation, shading systems and HVAC equipment. It was previously successfully applied to assess risks from climate change to cultural heritage assets and indoor collections (Leissner et al., 2015).

Overheating is one of the most significant problems with rising temperatures and will be one of the main foci of this article. In Germany, building components in refurbished buildings must comply with the U-values specified in the Building Energy Act (GEG (2020), which replaced the German Energy Saving Ordinance (EnEV) in 2020). In the future, a lower U-value of building components can be expected for energy saving. Typical measures to mitigate overheating include changing ventilation and adding shading. Considering the insulation, infiltration, ventilation habits and shading conditions of the currently tested house as a “baseline”, we have selected some potential measures to mitigate overheating, the effect of which is investigated in a later section (3.2.1). The selected potential measures are listed and explained below.

**Shading:** The shading of windows can effectively reduce the contribution of solar radiation indoors. Winkler et al. (2017) have shown that dynamic considerations are important for modeling operable window shades. The test house in this work (test house 2) is without any shading devices. To illustrate the effect of shading, a simulation was carried out in Section 3.2.1 assuming an additional shading device that operates at an indoor air temperature set point of 24 °C, reducing the solar gains by 50%.

**Ventilation:** Another measure is to increase the ventilation rate depending on the difference between indoor and outdoor temperatures. As an example, forced ventilation with an air change rate of 4 h<sup>-1</sup> was applied to the test house in Section 3.2.1 when the indoor air temperature is above 24 °C and the outdoor air temperature is below the indoor air temperature.

**Insulation:** the thermal properties of the building envelope are likely to be improved in the future, such as insulation and airtightness. Taking this future influencing factor into account, the thermal properties of our test house were also changed in Section 3.2.1: the insulation of exterior walls was improved to a U-value of 0.1 W/m<sup>2</sup>·K; for window glazes, the U-value was set to 1.1 W/m<sup>2</sup>·K, which is a high-performing double-glazed window, and the solar heat gain coefficient was reduced from 0.7 to 0.5.

**Airtightness:** measures to improve airtightness, e.g. sealing windows, will reduce air exchange. To illustrate this effect, in Section 3.2.1 we set the infiltration rate constant at 0.5 h<sup>-1</sup> and there was no more partial window opening time.

### 2.4. Parameters for the air quality simulation

The present work will mainly address indoor gas-phase air pollutants. In the current version of the IAQCC model, a limited number of organic compounds and gas phase reactions have been selected to describe commonly observed situations and/or health concerns. These 12 selected compounds cover the substance groups of VVOCs, VOCs, and SVOCs (very volatile, volatile, and semi-volatile organic compounds).

Provided the room air is well mixed, the general equation of the concentration of an indoor gas pollutant can be calculated as follows,

$$\frac{dC_{in}}{dt} = P \cdot \lambda \cdot C_{out} - \lambda \cdot C_{in} - \lambda_d \cdot C_{in} + \sum_{i=1}^n \frac{SER_{A,i} \cdot A_i}{V} + \sum_{i=1}^n \frac{SER_{u,i}}{V} \pm \psi_{gas} \quad (1)$$

where,  $C_{in}$  and  $C_{out}$  are the indoor and outdoor concentrations of one gas compound.  $P$  is the outdoor penetration factor,  $\lambda$  is the air change rate (h<sup>-1</sup>), and  $\lambda_d$  is the deposition rate of a species onto indoor surfaces (h<sup>-1</sup>). The release of a pollutant from the source  $i$  is represented as either an area-specific emission rate ( $SER_{A,i}$ ) or as a unit-specific emission rate ( $SER_{u,i}$ ).  $A_i$  is the area of the emission source  $i$  (m<sup>2</sup>), and  $V$  is the room volume (m<sup>3</sup>).  $\psi_{gas}$  is the production or removal rate via gas phase reactions. In the IAQCC model, temperature-dependent gas-phase reactions with ozone and OH radicals are treated using the well-documented examples of limonene and isoprene (Salthammer et al., 2022).

The outdoor concentration data of gaseous and particulate pollutants can be used to drive the model as external input files with user-defined timesteps, including ozone, preselected gas pollutants, particle number size distribution with user-defined particle size fraction, PM<sub>2.5</sub> and PM<sub>10</sub>. The initial concentrations of outdoor gas pollutants were taken from the literature (see Table S1 in the Supporting Information) (Geiss et al., 2011; Hellén et al., 2012; Nussbaumer et al., 2021). The initial diurnal variation of outdoor ozone (Fig. 2) was based on historical data from monitoring stations (1984–2007) in urban and rural areas in Germany (Melkonyan and Kuttler, 2012). The diurnal variations in outdoor OH radical concentrations were obtained from measured data near London (Emmerson et al., 2007), where the concentration ranged from 2.5·10<sup>5</sup>–2.5·10<sup>6</sup> molecule·cm<sup>-3</sup>. The diurnal variations are also consistent with measurements in Central Europe (Holland et al., 1998, 2003). Furthermore, Rohrer and Berresheim (2006) analyzed long-term measured data of atmospheric OH concentrations between 1999 and 2003 in Germany and found no detectable seasonal or annual trend for OH during the measurement period.

For naturally ventilated households, the air exchange between indoor and outdoor spaces takes into account the status of the windows (open/closed) and the infiltration through the building envelope. Residential air change rates  $\lambda$  usually range from 0.1 to 4 h<sup>-1</sup>, with a typical value of 0.5 h<sup>-1</sup> (Nazaroff, 2022). Zhao et al. (2020) reported ventilation rates in 40 German households, with mean air change rates of 0.2 h<sup>-1</sup> and 3.7 h<sup>-1</sup> for closed and open windows, respectively. For mechanically ventilated residential spaces, the U.S. national consensus standard ASHRAE Standard 62 specifies a minimum ventilation rate of 8.5 m<sup>3</sup> h<sup>-1</sup> (5 cubic feet per minute) per occupant (American Society of Heating Refrigerating and Air-Conditioning Engineers, 2022). Different filter options were also considered for aerosol particles in the IAQCC model, where corresponding particle size-resolved penetration factors  $P$  can be applied. As for gas compounds,  $P$  was assumed to be 1 (Terry et al., 2014).

Deposition rates  $\lambda_d$  of indoor ozone and OH were calculated by their deposition velocities (cm s<sup>-1</sup>) and the ratio of indoor surface area to volume  $A/V$  (m<sup>2</sup> m<sup>-3</sup>), where  $A$  considers the total surface area of the walls, floor, ceiling and furniture in indoor spaces. Deposition velocities for ozone (0.036 cm s<sup>-1</sup>) and OH (0.007 cm s<sup>-1</sup>) were taken from Sarwar et al. (2002).

The indoor emission sources include occupant activities (e.g. cook-

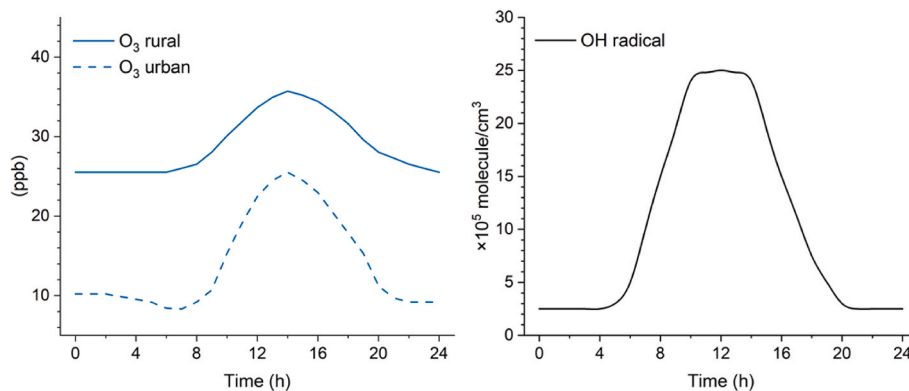


**Fig. 2.** Diurnal variation of outdoor ozone and OH radicals used in the model simulation for the central Europe region. Ozone data are historical average concentrations from monitoring stations (1984–2007) in Germany published by Melkonyan and Kuttler (2012) (1 ppb = 1.96  $\mu\text{g m}^{-3}$  at  $p = 1013$  hPa,  $T = 298$  K), and OH data were measured near London and published by Emmerson et al. (2007).

ing, burning candles, using air sprays) as well as furniture and building materials. As described in our previous work (Salthammer et al., 2022), the area-specific emission rates for materials were calculated by an empirical approach with a first-order exponential model. Emission characteristics of indoor furniture and building materials commonly used on the German market were analyzed on the basis of general emission data available at Fraunhofer WKI. The decay functions of the area-specific emission rates of the selected compounds for different materials applied in this work are summarized in Table S2 in the Supporting Information. By applying the desired material surface area  $A_i$ , the indoor emission of gas compounds can be reproduced for each specific house setting. In addition, the temperature-dependent emission rates of indoor furniture and materials were considered for the compounds for which data are available (see Table S3 in Supporting Information).

The air quality relevant pollutants in this paper include ozone, limonene, and mold. According to the World Health Organization's Air Quality Guidelines (2021b), the recommended air quality guideline (AQG) level for the short-term daily maximum 8-hour mean O<sub>3</sub> concentration is 100  $\mu\text{g m}^{-3}$ . The recommended AQG level for long-term exposure to O<sub>3</sub> is much lower at 60  $\mu\text{g m}^{-3}$ . For limonene, indoor guide values are available from the German Environment Agency (Umweltbundesamt – UBA), which has published two types of indoor guide values for various pollutants: Guide Value I (GVI) and Guide Value II (GVII) (Fromme et al., 2019). If the concentration of a substance in indoor air exceeds the GVI, preventive measures must be taken. GVII is an impact-related value based on current toxicological and epidemiological knowledge of a substance's impact threshold. Therefore, if the concentration of a substance in indoor air reaches or exceeds this level, immediate action must be taken. The GVI and GVII guide values for limonene are 1.0  $\text{mg m}^{-3}$  and 10  $\text{mg m}^{-3}$ , respectively. For mold exposure, however, there is not yet a guideline value. The "WHO Guidelines for Indoor Air Quality: Dampness and Mold" (World Health Organization, 2009) states that the relationship between microbial contamination and health effects cannot be accurately quantified and that no quantitative, health-based guidelines or thresholds for acceptable levels of contamination by microorganisms can be recommended.

### 2.5. Evaluation of the indoor comfort

The perceived comfort in indoor spaces is evaluated as a post-processing module in IAQCC. The perceived comfort was evaluated using the Predicted Mean Vote (PMV) and Predicted Percentage of Dissatisfied (PPD) model (Fanger, 1970), which takes into account an individual's metabolic rate, clothing insulation, and environmental conditions. PMV predicts how warm/cold a group of occupants is on a seven-point scale of thermal sensation, and PPD quantifies the

percentage of people in a large group of occupants exposed to the same thermal conditions who feel too warm or too cold. In this work, the PMV/PPD values were calculated using RStudio (Package *comf* version 0.1.11). The time series of the mean indoor surface temperature, the indoor air temperature and the relative humidity are taken as input from the results of the building simulation. In addition, data on air velocity and individual parameters (including clothing insulation and metabolic rate) are required. It was assumed that the occupant achieves thermal neutrality when the heat generated by the body's metabolism is dissipated and the body remains in thermal equilibrium with the environment. The insulating properties of clothing can be expressed in units of "clo". One clo unit is equal to 0.155 ( $\text{m}^2\cdot\text{K}/\text{W}$ ) of resistance. Although the unit "clo" is officially outdated, it is still often used in practice (Salthammer and Morrison, 2022). Energy expenditure caused by physical activity that exceeds energy expenditure at rest can be expressed in terms of metabolic equivalents (met) (McArdle et al., 2014). The values for insulation of different types of clothing and metabolic rates for different activity levels are provided in ISO/DIS 7730 (2023) and ASHRAE Standard 55 (American Society of Heating Refrigerating and Air-Conditioning Engineers, 2020).

In the assessment of this work, a person with a clothing insulation of 0.7 clo (e.g. T-shirt and long trousers) and a metabolic rate of 1 met was assumed. The air velocity was assumed to be 0.1  $\text{m s}^{-1}$ . The ASHRAE Standard 55 (2020) recommends PMV between  $-0.5$  and  $0.5$  and PPD  $<10\%$  as the comfortable thermal range. Based on this threshold, we define that PMV  $>0.5$  and PPD  $>10\%$  are considered "too warm". The percentage of time per year that this person feels "too warm" in the test house was then calculated.

A discomfort index (DI) is useful to evaluate the thermal stress people can experience. Several calculation methods are available for calculating DI (Salthammer and Morrison, 2022). We applied equation (2) as defined by Giles et al. (1990) because there is a direct relationship to the air temperature  $T_{\text{air}}$  (in  $^{\circ}\text{C}$ ) and the relative humidity RH.

$$DI = T_{\text{air}} - 0.55 \cdot (1 - 0.01 \cdot RH) \cdot (T_{\text{air}} - 14.5) \quad (2)$$

The DI values can be classified as follows:  $21 < DI < 29$  as increasing thermal discomfort and  $29 < DI < 32$  as severe heat stress (Epstein and Moran, 2006; Giles et al., 1990).

### 2.6. Evaluation of the indoor mold risk

The IAQCC model is able to simulate the heat transport in a thermal bridge and calculate the resulting surface temperature. Assuming well-mixed indoor air with uniform water vapor partial pressure, the relative humidity is calculated. The IAQCC applies a quasi-dynamic method using a temperature factor ( $f$ ) to calculate the surface temperature at thermal bridges neglecting storage effects, where  $f$  is the ratio between

the temperature difference of indoor air and indoor surface temperature and the temperature difference of indoor and outdoor air temperature. The mold growth risk was determined based on the VTT (Technical Research Centre of Finland) mold model, which provides a mold growth index with six categories (0–6) describing the intensity of growth on the surface of different building materials (Hukka and Viitanen, 1999; Viitanen et al., 2015). A mold growth index of 0 means no mold growth; between 1 and 3, mold can be seen under the microscope; >3, mold can be seen by the human eye (see Table S4 in the Supporting Information for details).

### 2.7. Future climate scenarios and pollutant concentrations

The IPCC Sixth Assessment Report (2021) assesses the climate response to five illustrative scenarios that cover the range of possible future greenhouse gas (GHG), land use and air pollutant development. Depending on the different GHG emission scenarios, the long-term (2081–2100) change in global surface temperature compared to the present (reference period 1995–2014) is very likely to be between +0.2 and +4.9 °C. The IPCC WGI Interactive Atlas further provides regional projections for various atmospheric variables under different scenarios and baseline conditions, including surface temperature, precipitation, as well as concentrations of air pollutants such as ozone and PM<sub>2.5</sub> (Gutiérrez et al., 2021; Iturbide et al., 2021).

Three Shared Socio-economic Pathway (SSP) scenarios from the IPCC projections were selected in this work: SSP1-2.6, SSP2-4.5, and SSP5-8.5, covering the low, medium, and very high levels of GHG emissions, respectively. The SSP5-8.5 scenario is later also referred to as the worst-case scenario. The geographic region of interest for this work is Western and Central Europe. It should be noted that the annual variations in mean surface temperature have been taken into account, whereby in summer the temperature increases more than in winter (the difference is greatest in the worst-case scenario, up to 3 °C).

The initial weather data near Braunschweig is taken from the Test Reference Year (TRY) data published by Deutscher Wetterdienst (DWD (2023), reference coordinates WGS84, access date 2022.12.07). TRY datasets were created based on a statistical analysis of real measured weather data for the period from 1995 to 2012 (current TRY). Hourly time series of the current TRY temperature and relative humidity are illustrated in Fig. S1. The dataset includes a spatial resolution of 1 km<sup>2</sup> and a temporal resolution of 1 h (Krähenmann et al., 2016). Based on this data, future ambient temperature is generated under different scenarios. Ambient RH is assumed to be the same as current (annual mean = 72%), due to the lack of data and relatively high uncertainty in predicting future trends (Dunn et al., 2017).

For future outdoor ozone concentrations, due to different climate models and assumptions, there are conflicting predictions in the literature for the European region. Some predict a declining trend (Coelho et al., 2021; Colette et al., 2012, 2013; Karlsson et al., 2017; Langner et al., 2012; Watson et al., 2016), others an increasing trend (Giorgi and Meleux, 2007; Meleux et al., 2007; Melkonyan and Wagner, 2013). The decreasing trend is broadly based on the assumption of a decrease in emissions of ozone precursors. Consistent with the future climate projection, we used the ozone prediction from the IPCC WGI Interactive Atlas (Gutiérrez et al., 2021; Iturbide et al., 2021), which predicts both decreasing and increasing trends in the ozone concentration depending on different scenarios. Note that the prediction in the IPCC SSP scenarios only provides the change in annual mean concentration. We then added the concentration changes to the diurnal variation using measured historical ozone concentrations (see Fig. 2) for the corresponding future year. As for future outdoor OH radicals, current values were assumed due to a lack of data. In addition, the chemical lifetime of OH is so short that changes caused by physical processes such as transport from outdoors to indoors and deposition on the surface can be neglected (Carlaw, 2007).

## 3. Results and discussion

### 3.1. Future trend of indoor climate and pollutants in Central Europe: the most likely scenarios

#### 3.1.1. Indoor climate and thermal comfort

Long-term simulations of indoor climate and indoor air quality parameters from 2020 to the year 2100 were performed for the test house (“baseline” settings) under the three future scenarios with a temporal resolution of 1 min. The resulting annual trend and annual variation for each are presented and discussed in this section.

The annual average outdoor temperatures from 2020 to 2100 under three SSP climate scenarios are shown in Fig. 3a. The long-term predicted mean annual change in surface temperature is 0.8 °C, 2.2 °C and 5.5 °C for scenarios SSP1-2.6, SSP2-4.5 and SSP5-8.5, respectively. The simulated annual mean indoor air temperature for the test house (“baseline” settings) is 19 °C in 2020. By 2100, the indoor temperature increases by 0.5, 1.2 and 3.4 °C for the scenarios SSP1-2.6, SSP2-4.5 and SSP5-8.5, respectively (Fig. 3b). As the indoor temperature rises, the RH also increases accordingly. It is important to note that the summertime mean indoor temperatures show a more significant increase, by 0.9, 2.5 and 6.4 °C, respectively. This can be attributed to the greater increase in the outdoor temperature, the higher ventilation rate, as well as the solar radiation in summer considered in the building simulation model (Erhardt and Antretter, 2012). In the next section, future indoor overheating and air quality on hot summer days are examined in more detail.

The perceived indoor comfort (PMV/PPD) was calculated using the simulated minute surface temperature, the air temperature and the relative humidity values in the test house. As shown in Fig. 3d, in 2020 people barely feel “too warm”. In 2100, there is only a slight increase in the amount of time feeling “too warm” under the SSP1-2.6 scenario. Under the worst-case scenario (SSP5-8.5), however, people will feel “too warm” for more than 35% of the time in 2100.

Theoretically, the PMV model predicts well the thermal sensation of people in temperature-controlled environments, and an adaptive comfort model may be more suited to evaluate the times in lower comfort categories due to overheating (Carlucci et al., 2018). Nevertheless, we chose the PMV model because it is a widely used approach and its thermal comfort assessment results are sufficiently robust for comparison under different future scenarios, taking into account the uncertainties of temperature and humidity in the future climate assumptions. The approach we present is intended to be applicable to non-air-conditioned and air-conditioned buildings, as the building physics model can fully control the heat and moisture transport as well as the type and profile of ventilation of the simulation building. Therefore, the PMV model made sense and was considered first in the model development. However, an evaluation using an adaptive model for thermal comfort will be beneficial and will be added in a future revision of the model.

With the temperature and relative humidity levels simulated for the year 2100 under three SSP scenarios, the DI values in the test house were calculated using equation (2). Fig. 4 shows hourly averages and it is obvious that under the worst-case scenario, the occupants will suffer from thermal discomfort from May to October. Moreover, five of the days have DI values above 29, which means that people will suffer severe heat stress. Under the scenarios SSP1-2.6 and SSP2-4.5, the occupants also perceive thermal discomfort but no heat stress.

#### 3.1.2. Mold risk

Under certain combinations of indoor temperature and humidity, the risk of mold growth on building surfaces increases. The mold index was calculated under the simulated indoor climate of the test house on different thermal bridge materials with different temperature factors in the long term (year 2100). Note that an internal heat and moisture load of two people sitting quietly is assumed here, which is a different but still realistic scenario compared to the example case in our earlier work

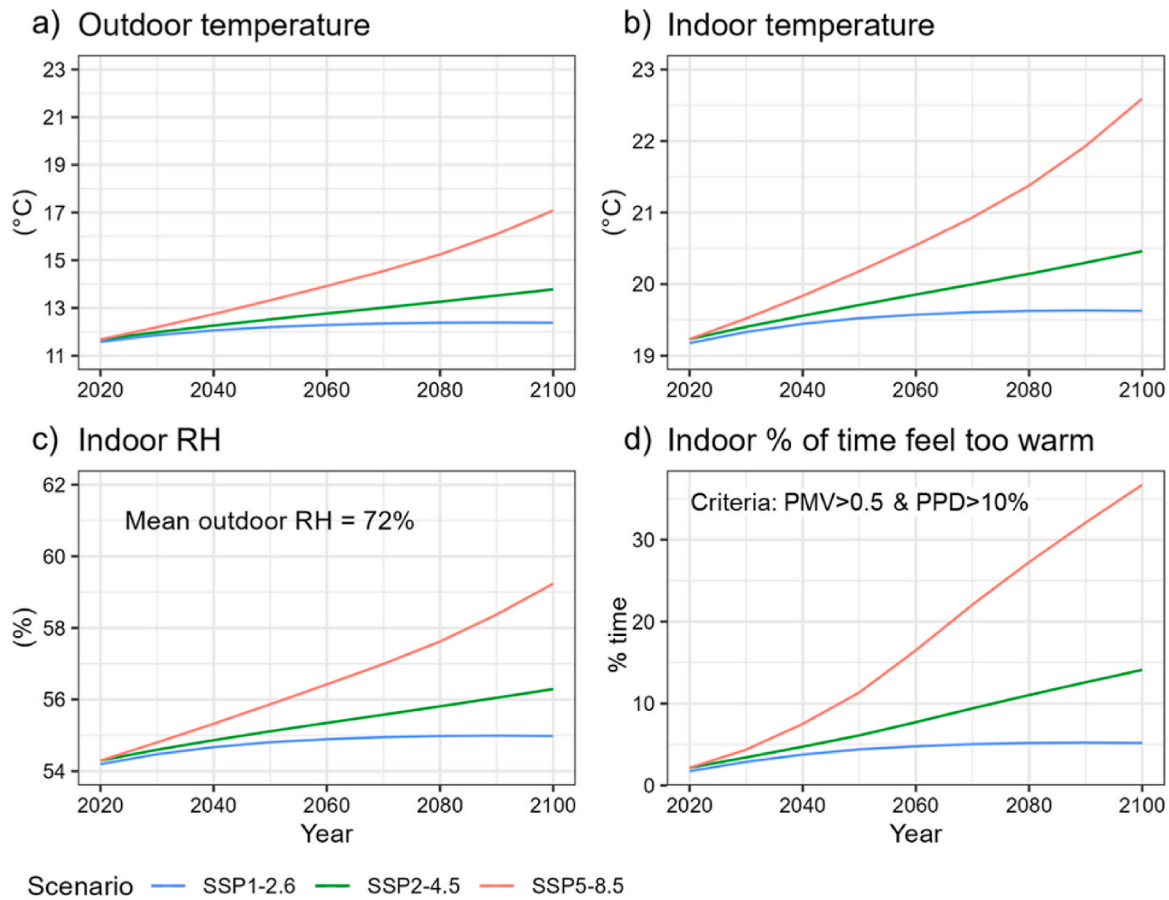


**Fig. 3.** Annual average of simulated indoor climate in the test house from 2020 to 2100 under three SSP climate scenarios for Western and Central Europe region. a) Estimated outdoor temperature, b)-c) Simulated indoor air temperature and relative humidity (RH), and d) The percentage of time per year that people feel “too warm”, criteria: Predicted Mean Vote (PMV) > 0.5, Predicted Percentage of Dissatisfied (PPD).

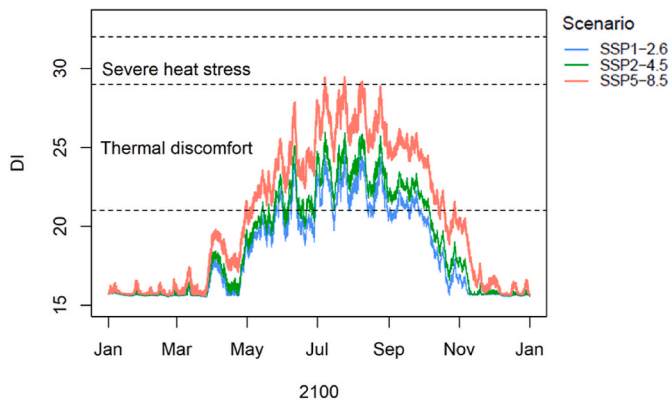


**Fig. 4.** Time course of the discomfort index (DI) in the test house in 2100 (hourly means) under different SSP scenarios.

(Salthammer et al., 2022) where much higher internal loads from 5 people were assumed. In Germany, the minimum temperature factor ( $f$  value) allowed for new or renovated buildings is 0.7 (DIN 4108-2, 2013). For the test house condition, at a  $f$  of 0.7, even very sensitive material (e.g. pine sapwood) will not develop any significant mold in the long term.

Assuming our test house is not renovated, worse insulation and lower  $f$  can be expected. We therefore also applied  $f = 0.5$  for the simulation as an example. Fig. 5 shows the simulated mold growth index over two

years with hourly resolution. One can see the annual variation in the risk of mold growth on indoor surfaces, where the mold risk reaches a peak in the winter and decreases in the summer. Due to the small temperature difference under the SSP1-2.6 scenario, the predicted mold index in the long term is very similar to those of 2020 and no significant mold growth can be found even for very sensitive materials. For thermal bridges of sensitive materials (e.g. wood paneling) and medium resistant materials (e.g. concrete), mold would not be an issue in the simulated climate of the test house under different future scenarios. However, for very sensitive materials, a mold risk is expected in the long term for the SSP2-4.5 and SSP5-8.5 scenarios.

### 3.1.3. Indoor gas-phase air pollutants

In order to illustrate the gas-phase degradation of reactive VOCs with ozone or OH radicals, simulated long-term indoor limonene concentrations in the test house are presented and discussed in the following.

As with the indoor climate simulation, indoor air pollutants are simulated with a resolution of 1 min and presented as hourly or annual averages. Based on the IPCC WGI Interactive Atlas projection (Gutiérrez et al., 2021; Iturbide et al., 2021), future outdoor ozone concentrations show a decreasing trend for the SSP1-2.6 and SSP2-4.5 scenarios and an increasing trend for the SSP5-8.5 scenario (see Fig. 6). In 2020, the simulated annual mean indoor ozone concentration is 4.9 ppb (corresponding to around  $9.8 \mu\text{g m}^{-3}$ , assuming  $p = 1013 \text{ hPa}$ ,  $[\mu\text{g m}^{-3}] = [\text{ppb}] \cdot (12.187) \cdot (\text{MW}) / (273.15 + T_{\text{air}})$ , where MW represents the molecular weight in  $\text{g mol}^{-1}$  and the unit of  $T_{\text{air}}$  is  $^{\circ}\text{C}$ ). This value is within the expected range of typical indoor ozone concentrations (4–6 ppb, as described by Nazaroff and Weschler (2022)). The future annual trend of

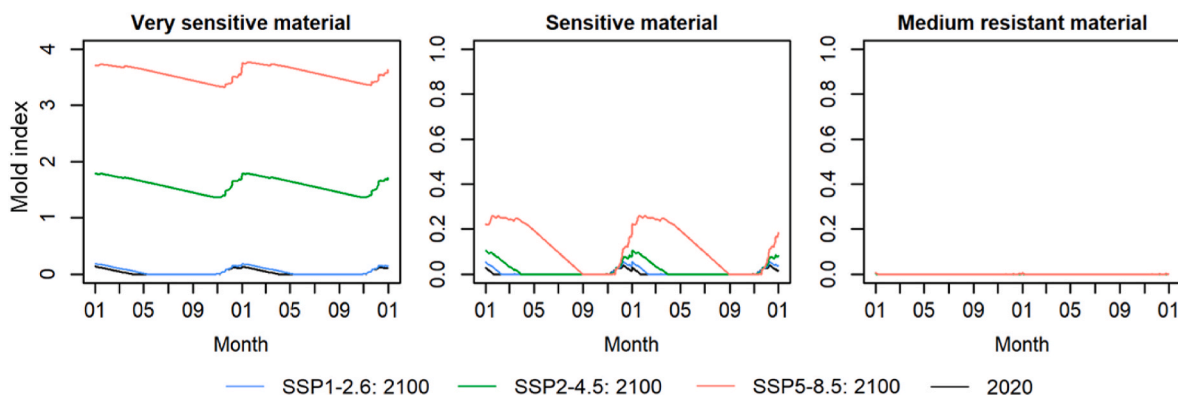


Fig. 5. Comparison of the predicted mold index for different thermal bridges with a temperature factor  $f = 0.5$  in the test house for the year 2020 and for the year 2100.  $f$  is the ratio between the temperature difference between indoor air and indoor surface temperature and the temperature difference between indoor and outdoor air temperature. Medium resistant material is not expected to develop mold and thus is consistently 0.

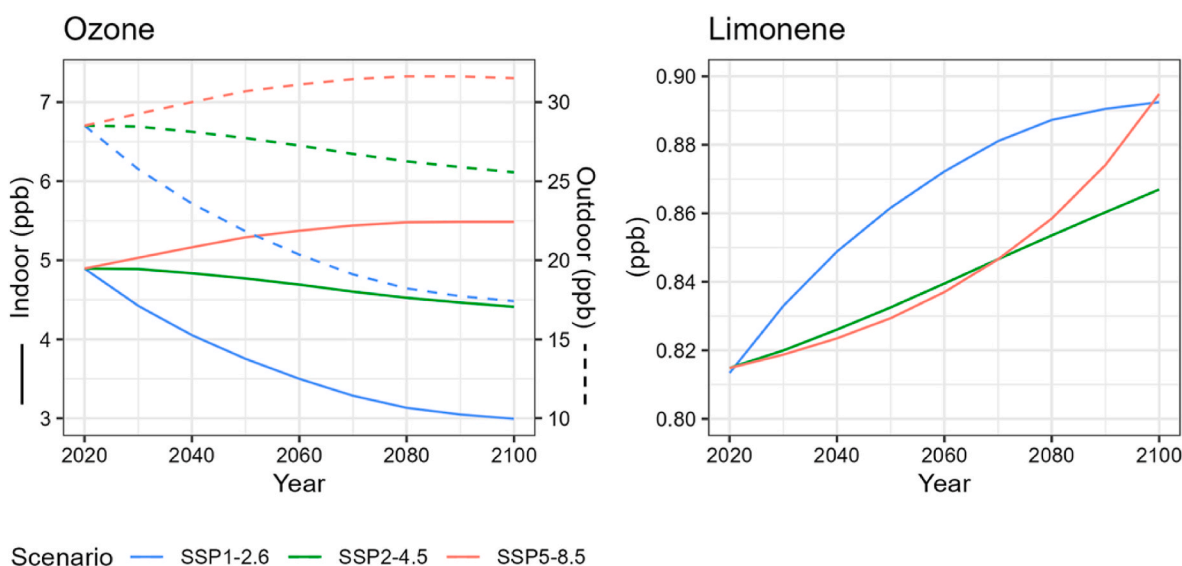


Fig. 6. Future trend of annual mean indoor ozone and limonene concentration in the test house from 2020 to 2100 under three SSP climate scenarios for Western and Central Europe region. The dotted line represents outdoor ozone concentrations.

indoor ozone concentrations follows that of outdoor air. By 2100, the annual mean indoor ozone concentrations are 3.0, 4.9, and 5.5 ppb for the SSP1-2.6, SSP2-4.5, and SSP5-8.5 scenarios, respectively. In summer, indoor ozone concentrations are often higher than in winter, which is due to higher ventilation rates. The average indoor ozone concentration in summer (June–August) is 8.8 ppb in 2020 and 10 ppb in 2100 under the worst-case scenario.

A higher ozone concentration can lead to a lower concentration of reactive VOCs. However, as shown in Fig. 6, despite the increasing or decreasing trend of indoor ozone concentration, indoor limonene levels continue to increase under different future scenarios. This can be attributed to the increasing emission rate of limonene from furniture and building materials due to the temperature increase, which cannot be compensated by the increasing reaction rate with ozone (Atkinson and Arey, 2003). As the annual mean indoor temperature increases in 2100 (see Fig. 3b), the mean annual limonene emission rate increases by 9, 25 and 66  $\mu\text{g h}^{-1}$ , respectively. This effect is particularly pronounced on summer days with extreme temperature rises. In the next section, the indoor limonene-ozone response on future summer days is discussed in detail.

### 3.2. Case study of extremely hot weather in Central Europe on a long-term horizon

In order to better understand what can be expected under extreme conditions of climate change, the summer days in the worst-case scenario are examined in detail in the long term. The test house settings are described in Section 2.2, and the assumptions of future outdoor climate and pollutant concentrations are described in Section 3.1.

#### 3.2.1. Indoor overheating and mitigation measures

Since the test house is located in Germany, we applied the German standard DIN 4108-2 (2013) for the evaluation of overheating. This standard provides criteria for the thermal protection of buildings based on the indoor operative temperature. The operative (or perceived) temperature is defined as the uniform temperature of a space in which an occupant would exchange the same amount of heat by radiation and convection as in the existing non-uniform environment. Operative temperature is a simplified measure of human thermal comfort derived from air temperature and the mean radiant temperature (ISO/DIS 7730, 2023).

The standard DIN 4108-2 (2013) also divides Germany into three different regions, considering the regional differences in summer climate conditions, each with different reference values for the indoor

operative temperature above which overheating needs to be considered. The three regions include A. the low mountain range or coastal region, C. river lowlands such as the Rhine valley, and B. the rest of most areas in Germany. Braunschweig is located in summer climate region B (average climate), which defines the reference value for overheating at an operative temperature of 26 °C. The degree-hours above this reference value are summed up for the whole year. Degree-hours is a simple metric that can be used to measure how much (in degrees), and for how long (in hours) the actual operative temperature exceeds the reference value. A required maximum value of 1200 Kh/a (annual sum of 'Kelvin \* hours') shall not be exceeded.

The indoor operative temperature was simulated for the summer period from May 1 to October 1 under four different climate scenarios: the year 2020 and the year 2100 under SSP1-2.6, SSP2-4.5, and SSP5-8.5 scenarios. The current test house settings regarding insulation, infiltration, ventilation habits and the shading condition are treated as the "baseline" scenario. Simulations were also performed for various combinations of measures that could be applied to the test house to determine their effects, including ventilation, shading, insulation and airtightness (explained in Section 2.3). Table 1 shows a summary of all the overheating degree-hours for the selected mitigation measures for all climate scenarios.

For the baseline case, i.e. without any measures, the degree-hours in 2020 are 568Kh/a, which is below the threshold of 1200Kh/a, while in 2100, the "degree-hours" exceed this threshold even in the SSP1-2.6 scenario. Once any of the selected mitigation measures are applied, the threshold is no longer exceeded in the SSP1-2.6 scenario, except for an insulated, airtight building where no additional shading or ventilation is applied. As expected, this case (i.e. only improving insulation and airtightness) shows the lowest performance in general and would already exceed the threshold under today's climate with 1573 Kh/a simulated. The efficiency measures applied can only achieve their benefits when combined with means to control solar gains (i.e. shading) and/or means to remove excess heat in the space (i.e. ventilation). With a combination of insulation, airtightness, shading and ventilation we see the lowest degree-hours of all cases. However, under the worst-case scenario (SSP5-8.5), the threshold is still exceeded with 3306 Kh/a.

In this example, the measure of adjusting ventilation (i.e., active forced ventilation with an air change rate of 4 h<sup>-1</sup> when the outdoor temperature is lower than the indoor temperature), is more effective in keeping the indoor temperature within an acceptable range than shading the windows. Even in climatic situations with long periods of high temperatures, taking advantage of the temperature difference due to the diurnal cycle is still a possibility under the climatic conditions of Germany. It is important to note that, this conclusion is drawn on the basis of the climate change prediction considered in this paper. Fischer and Schär (2010) expect an increase in tropical days (temperature >35 °C) and nights (temperature >20 °C) of up to 6 days/year for Germany by the end of the 21st century. Under this assumption, in the long term, adjusting ventilation alone will not be sufficient to cope with

**Table 1**  
Overheating indoors as degree-hours (Kh/a) under different climate scenarios with various mitigation measures for the test house, including ventilation, shading, insulation and airtightness (for details see Section 2.3).

Measures	Scenarios			
	2020	2100 (SSP1-2.6)	2100 (SSP2-4.5)	2100 (SSP5-8.5)
Baseline	568	1254	3068	11 939
Insulation + Airtightness	1573	1936	6115	16 668
Shading	69	318	1418	8184
Ventilation	11	84	526	4473
Ventilation + Airtightness	13	77	535	4477
Ventilation + Shading	0	17	266	3541
Insulation + Airtightness + Ventilation + Shading	0	6	189	3306

the persistent tropical weather.

### 3.2.2. Indoor gas reaction

Indoor air pollutant concentrations and reactions in the test house ("baseline" settings) were simulated for a typical summer day in 2020 and 2100 under the worst-case scenario (SSP5-8.5) with a 1-min resolution. The results of the diurnal time series of indoor and outdoor temperature, ozone, indoor limonene and OH radicals are illustrated in Fig. 7.

In this summer day example, the daily variation in outdoor air temperature is up to 10 °C, while the indoor temperature is much more stable with a difference between the maximum and minimum temperature of one degree for both cases (Fig. 7a). As this work focuses on the response of buildings to future climate, emissions from residential activities are not included in the simulations, which results in lower emissions of VOCs than in the real-world scenario. In our simulations, the only indoor emission source of limonene is furniture. The simulated room in the test house has an estimated furniture area of 135 m<sup>2</sup>, including 50 m<sup>2</sup> of soft furniture and 85 m<sup>2</sup> of wooden furniture. Assuming that the changes in the emission strength of furniture are driven only by temperature, the temperature-dependent emission rates of limonene from wooden furniture can be calculated using the area-specific emission rate data and the temperature-dependent coefficient (Table S2 and Table S3). It should be noted that to avoid the influence of other processes such as degradation and abrasion on limonene emissions, the same conditions were assumed for the furniture for 2020 and 2100. As shown in Fig. 7b, the simulated limonene emission rate follows the trend of diurnal variations in indoor air temperature. Furthermore, the indoor air temperature difference (about 7°) in 2020 and 2100 leads to the mean limonene emission rate increase from 625 µg h<sup>-1</sup> to 760 µg h<sup>-1</sup>.

In both cases, diurnal variation in the indoor ozone concentration can be clearly seen, ranging from 7.8 to 10.8 ppb and 9–12.2 ppb in 2020 and 2100, respectively. The daily maximum 8-hour mean O<sub>3</sub> concentrations in both cases are below the short-term guideline value 100 µg m<sup>-3</sup> (equivalent to 51 ppb at 298 K and 1013 hPa) of the World Health Organization's Air Quality Guidelines (World Health Organization, 2021b). The indoor O<sub>3</sub> concentrations increase and decrease almost simultaneously with the outdoor concentrations. More limonene is emitted during the day as the indoor temperature increases and consequently, more ozone is expected to be consumed via the gas phase reaction. However, this cannot compensate for the increased contribution of outdoor ozone due to higher ventilation. OH radicals are generated in the limonene-ozone reaction and consumed by the reaction with limonene; the resulting concentration ranges from 0.8·10<sup>-5</sup> ppb to 1.5·10<sup>-5</sup> ppb. As expected, indoor limonene concentrations are higher in 2100 than in 2020. However, the limonene concentration is rather low compared to other studies such as by Carslaw (2007, 2013) and Sarwar et al. (2002). Considering that the only source of limonene is furniture and no other residential activities, such as cleaning and use of air freshers, were included, the simulated concentration is still within a realistic range. The simulated indoor limonene concentrations in 2020 and 2100 are all below 1 ppb and thus far below the guideline values GVI (1.0 mg m<sup>-3</sup>) and GVII (10 mg m<sup>-3</sup>) (corresponding to 179 ppb and 1795 ppb, respectively, assuming p = 1013 hPa, T = 298 K) specified by the German Environment Agency (Fromme et al., 2019).

### 3.2.3. Validation of the indoor gas reaction

To further validate the performance of our model, the results were compared with the Indoor CHEMical model in Python (INCHEM-Py) developed by the Carslaw group (Shaw and Carslaw, 2021). INCHEM-Py is an indoor box model that follows the explicit chemical degradation of 135 volatile organic compounds using the Master Chemical Mechanism (Jenkin et al., 1997). It has a unique set of modules that specifically focus on the indoor gas-phase chemical reactions, including indoor photolysis parameterization, surface-dependent deposition of O<sub>3</sub> and

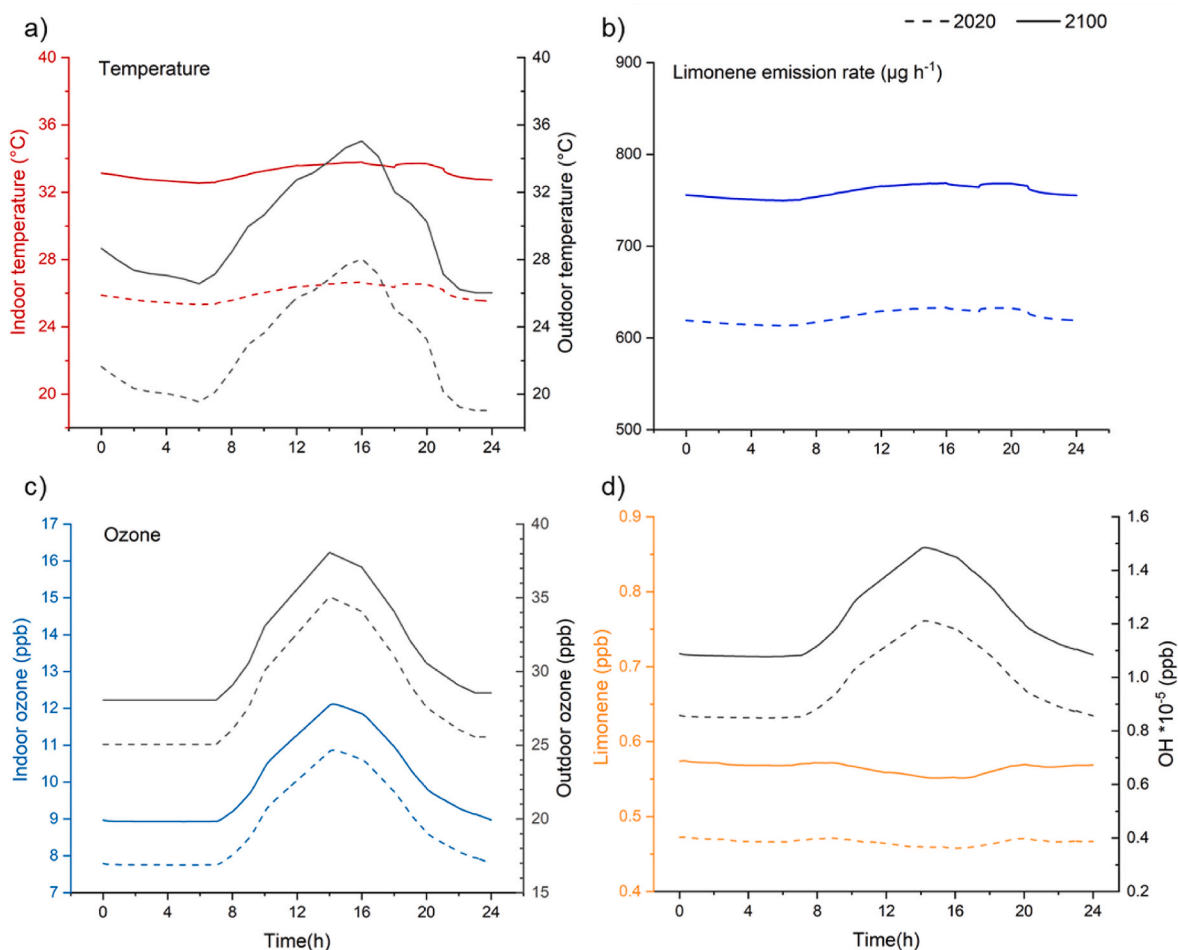


**Fig. 7.** Comparison of diurnal cycles of air parameters for a summer day in 2020 (dashed line) and 2100 (solid line) in the test house: a) estimated outdoor and simulated indoor air temperature, b) temperature-dependent indoor limonene emission rates from furniture, c) estimated outdoor and simulated indoor ozone concentrations, and d) simulated indoor limonene and OH radical concentrations. Limonene, ozone, and OH radical concentration calculated at  $p = 1013$  hPa (unit conversion using  $[\mu\text{g m}^{-3}] = [\text{ppb}] \cdot (12.187) \cdot (\text{MW}) / (273.15 + T_{\text{air}})$ ).

$\text{H}_2\text{O}_2$  and indoor-outdoor air exchange. The model is described in detail in Shaw et al. (2023). The full settings files for the model are included in the data attached to this paper and have duplicated the IAQC model where possible. When this was not possible, INCHEM-Py values were left as default, including 114 constant outdoor concentrations, including

limonene and isoprene, and 6 additional diurnal outdoor concentrations. The relative humidity was constant for both 2020 and 2100 at 50 % and the air change rate was set at  $1.5 \text{ h}^{-1}$  with diurnal concentrations for  $\text{NO}_2$ ,  $\text{HO}_2$ ,  $\text{CH}_3\text{O}_2$ , and HONO from measurements taken in suburban London (Shaw et al., 2023). Sunlight was attenuated from outdoors

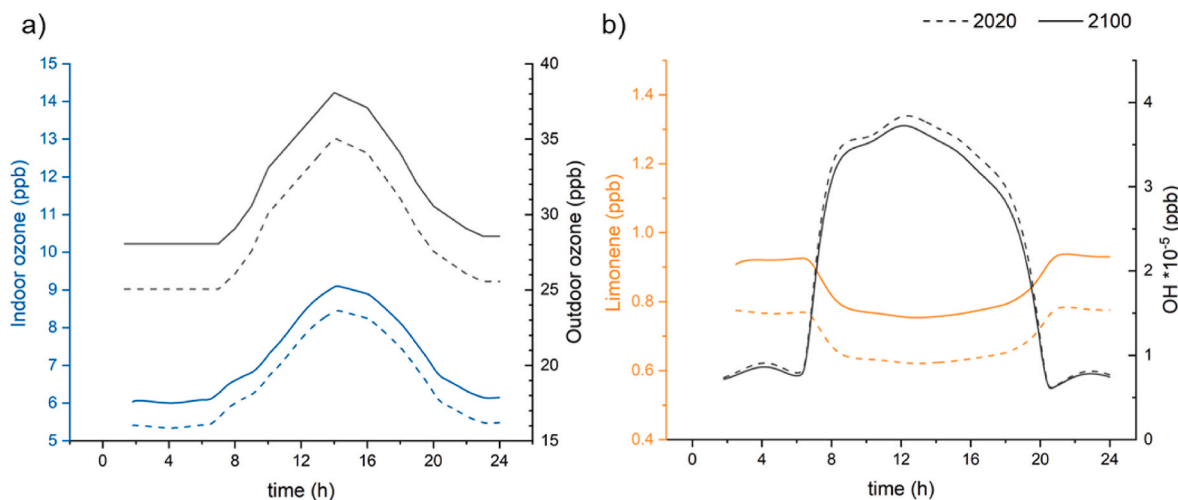


**Fig. 8.** Simulated concentrations of indoor a) ozone, and b) limonene and OH radical concentrations using INCHEM-Py.

using a high transmission glass, with a low wavelength cut-off of 308 nm (Sacht et al., 2016) as described in Wang et al. (2022), and no indoor lighting was used.

Results from INCHEM-Py show significantly more diurnal variation in the species concentrations than IAQCC, with limonene decreasing during the day through reactions with OH (see Fig. 8). The main driver of OH in INCHEM-Py is the reaction of HO<sub>2</sub> with NO to form OH and NO<sub>2</sub>, and VOC degradation reactions, which are not included in the IAQCC model. This also accounts for the higher O<sub>3</sub> in the IAQCC model as there are fewer VOCs included for O<sub>3</sub> to react with. As more VOCs are available to react with O<sub>3</sub> in INCHEM-Py there is less O<sub>3</sub> available to react with limonene, and consequently higher concentrations of limonene throughout.

Different from the indoor O<sub>3</sub> concentrations in the IAQCC model, values in INCHEM-Py start to increase at sunrise before the outdoor concentrations increase. This is due to the inclusion of photolysis in INCHEM-Py which creates O<sub>3</sub> indoors. Production of O<sub>3</sub> from O (from the photolysis of NO<sub>2</sub>) causes an increase in indoor O<sub>3</sub> at dawn. O<sub>3</sub> then follows the outdoor concentration with the peak indoor concentration being around 8 min behind the peak outdoor concentration. The outdoor O<sub>3</sub> concentration does drive the indoor concentration for the majority of the INCHEM-Py simulation, but additional production mechanisms are also important, compared to the simpler chemical scheme adopted in IAQCC.

With regard to the future development of ambient ozone concentrations, the IPCC report only provides for the change in the annual mean concentration, and this change seems to be rather small. However, several studies have shown that heat waves are often accompanied by extremely high ozone concentrations (Fischer et al., 2004; Lee et al., 2006; Pu et al., 2017; Vautard et al., 2005; Vieno et al., 2010). In the European Union, the Air Quality Directive 2008/EC/50 (EU, 2008) sets a concentration of 120 µg m<sup>-3</sup> (8-h average) as the target value and long-term objective value for ozone to protect human health. Salthammer et al. (2018) reported that from 2001 to 2016, the reference value was exceeded on average for 10–30 days for eight observed German cities (urban background). An outstanding exception is the heat wave year 2003, where the reference value was exceeded on more than 60 days. Assuming that outdoor ozone in the summer of 2100 will also show extremely high concentrations more frequently in the context of global warming, we applied the diurnal ozone data of Salthammer et al. (2018) to re-simulate the concentrations of indoor gaseous pollutants in the test house. The results show that indoor ozone concentrations can reach 26 ppb and 20 ppb when applying IAQCC and INCHEM-P, respectively (see Fig. S3 in the Supporting Information). In addition, in this example of a summer day simulation, the air change rate was set at 1.5 h<sup>-1</sup> because we assumed that the occupants kept the windows tilted. Once people widely open the windows, the air change rate can be much higher, and a higher indoor ozone concentration can be expected.

Overall, the IAQCC results show a reasonable agreement when compared to the explicitly detailed indoor chemistry model INCHEM-Py. Despite the limited number of compounds and reaction mechanisms, IAQCC provides a comprehensive and realistic estimate of indoor air pollutant concentrations. Indeed, IAQCC can capture the effects of outdoor contributions as well as the effects of temperature rise, even within a reasonable range, which is sufficient to provide reliable results for modeling the effects of climate change, especially given the uncertainty in expected future air pollutant concentrations.

#### 4. Conclusion

First, it should be stated once again, and in all clarity, that the IAQCC model is not intended to be used to accurately predict the future indoor climate of a particular region. Rather, it uses optimistic, realistic and pessimistic assumptions to estimate a range of likely long-term trends. Such results can help to identify suitable mitigation measures for the future.

It is increasingly unlikely that the exceedance of the 1.5 °C warming target for the planet can be avoided by the year 2100. Instead, we must be prepared for an average temperature increase of at least 2.0–2.5 °C, taking into account extreme heat waves, which we are experiencing more and more frequently in Europe. When evaluating the climate, regardless of whether it is indoors or outdoors, one should take equal account of temperature and humidity, as is also the case with the discomfort and heat stress indices. Humid air has a significantly higher enthalpy than dry air, which can be shown with simple thermodynamic calculations (Salthammer and Morrison, 2022).

The house used for the modeling in this work is a thermally insulated old building whose outer walls correspond to the current status of the German Building Energy Act (GEG, 2020) regulation for existing buildings, while the windows do not meet the actual requirement of the GEG. Nevertheless, we chose this house type because the insulation reflects the reality of new construction and retrofitting in Germany.

Our simulations show the expected continuous mean increase of all examined parameters, which is not surprising. Ozone concentrations could exceed critical levels more frequently in the future. However, most of the air pollutant concentrations can be limited relatively easily by choosing low-emission materials and products and by using intelligent ventilation concepts. The problem is temperature and humidity. In a well-insulated house by today's standards, thermal stress will be expected in the future (see Fig. 4) if additional measures are not taken. These primarily include shading and living behavior adapted to the climate (see Table 1).

It can therefore be expected that the current legal measures are a step in the right direction, but will not be sufficient in the long term. The realization that additional action and emergency plans are necessary is becoming apparent, but has not yet become established. Mechanical air conditioning may be necessary for certain house conditions in Central Europe, but this approach collides with the efforts to save energy and requires careful consideration with alternative passive options to reduce overheating. The IAQCC model allows for short- and long-term predictions of the effects of climate change on indoor climate, air quality and mold growth. While the exact consequences of future climate change on nature and society are unknown, one can still be prepared for a predictable future climate. The results can provide valuable insights for a more comprehensive and enhanced assessment of upcoming climate events, as well as more rigorous development of preventive and protective measures.

#### CRedit authorship contribution statement

**Jiangyue Zhao:** Conceptualization, Methodology, Software, Formal analysis, Writing - Original Draft, Writing - Review & Editing. **Erik Uhde:** Writing - Review & Editing. **Tunga Salthammer:** Conceptualization, Writing - Original Draft, Writing - Review & Editing, Supervision, Funding acquisition. **Florian Antretter:** Writing - Original Draft, Writing - Review & Editing. **David Shaw:** Writing - Original Draft, Writing - Review & Editing. **Nicola Carslaw:** Writing - Review & Editing. **Alexandra Schieweck:** Writing - Review & Editing, Supervision, Project administration, Funding acquisition.

#### Funding information

This work was supported by the Federal Ministry for the Environment, Nature Conservation, Nuclear Safety and Consumer Protection (BMUV), Germany [grant number REFOPLAN FKZ 3719 51 205 0].

#### Declaration of competing interest

The authors declare that they have no known competing financial interests or personal relationships that could have appeared to influence the work reported in this paper.

## Data availability

Data will be made available on request.

## Acknowledgment

The authors gratefully acknowledge the Federal Ministry for the Environment, Nature Conservation, Nuclear Safety and Consumer Protection (BMUV) grant REFOPLAN FKZ 3719 51 205 0 (title translated from German: "Influence of climatic change on indoor air quality: expert system, quantitative protections, and information system for the public"). The authors are also grateful to Manuela Lingnau (Fraunhofer WKI) for designing the graphical abstract.

## Appendix A. Supplementary data

Supplementary data to this article can be found online at <https://doi.org/10.1016/j.envres.2023.117804>.

## References

- American Society of Heating Refrigerating and Air-Conditioning Engineers, 2020. Standard 55 - Thermal Environmental Conditions for Human Occupancy. American Society of Heating, Refrigerating and Air-Conditioning Engineers (ASHRAE), Atlanta. <https://www.ashrae.org/technical-resources/bookstore/standard-55-thermal-environmental-conditions-for-human-occupancy>.
- American Society of Heating Refrigerating and Air-Conditioning Engineers, 2022. Standard 62 - Ventilation and Acceptable Indoor Air Quality. American Society of Heating Refrigerating and Air-Conditioning Engineers (ASHRAE), Atlanta. <https://www.ashrae.org/technical-resources/bookstore/standards-62-1-62-2>.
- F., Antretter, Pazold, M., Künzel, H.M., Sedlbauer, K.P., 2015. Anwendung hygrothermischer Gebäudesimulation. *Bauphysik Kalender 2015: Simulations- und Berechnungsverfahren*. WILEY-VCH, Weinheim, pp. 189–225. Chapter C3.
- Atkinson, R., Arey, J., 2003. Atmospheric degradation of volatile organic compounds. *Chem. Rev.* 103, 4605–4638. <https://doi.org/10.1021/cr0206420>.
- Brasseur, G.P., Jacob, D., Schuck-Zöllner, S., 2017. *Klimawandel in Deutschland*. Springer Spektrum, Berlin.
- Bund/Länder Ad-hoc Arbeitsgruppe Gesundheitliche Anpassung an die Folgen des Klimawandels, 2017. Handlungsempfehlungen für die Erstellung von Hitzeaktionsplänen zum Schutz der menschlichen Gesundheit. *Bundesgesundheitsblatt* 60, 662–672. <https://doi.org/10.1007/s00103-017-2554-5>.
- Carlucci, S., Bai, L., de Dear, R., Yang, L., 2018. Review of adaptive thermal comfort models in built environmental regulatory documents. *Build. Environ.* 137, 73–89. <https://doi.org/10.1016/j.buildenv.2018.03.053>.
- Carlslaw, N., 2007. A new detailed chemical model for indoor air pollution. *Atmos. Environ.* 41, 1164–1179. <https://doi.org/10.1016/j.atmosenv.2006.09.038>.
- Carlslaw, N., 2013. A mechanistic study of limonene oxidation products and pathways following cleaning activities. *Atmos. Environ.* 80, 507–513. <https://doi.org/10.1016/j.atmosenv.2013.08.034>.
- Coelho, S., Rafael, S., Lopes, D., Miranda, A., Ferreira, J., 2021. How changing climate may influence air pollution control strategies for 2030. *Sci. Total Environ.* 758, 143911. <https://doi.org/10.1016/j.scitotenv.2020.143911>.
- Colette, A., Bessagnet, B., Vautard, R., Szopa, S., Rao, S., Schucht, S., Klimont, Z., Menut, L., Clain, G., Meleux, F., 2013. European atmosphere in 2050, a regional air quality and climate perspective under CMIP5 scenarios. *Atmos. Chem. Phys.* 13, 7451–7471. <https://doi.org/10.5194/acp-13-7451-2013>.
- Colette, A., Granier, C., Hodnebrog, Ø., Jakobs, H., Maurizi, A., Nyiri, A., Rao, S., Amann, M., Bessagnet, B., d'Angiola, A., 2012. Future air quality in Europe: a multi-model assessment of projected exposure to ozone. *Atmos. Chem. Phys.* 12, 10613–10630. <https://doi.org/10.5194/acp-12-10613-2012>.
- DIN 4108-2, 2013. *Thermal Protection and Energy Economy in Buildings - Part 2: Minimum Requirements to Thermal Insulation*. Beuth Verlag, Berlin.
- Dunn, R.J., Willett, K.M., Ciavarella, A., Stott, P.A., 2017. Comparison of land surface humidity between observations and CMIP5 models. *Earth Syst. Dynam.* 8, 719–747. <https://doi.org/10.5194/esd-8-719-2017>.
- DWD, 2023. Location-specific Test Reference Year (TRY) Dataset 2017 - Climate Consulting Module. German Weather Service (DWD). [https://kunden.dwd.de/obf/\(2022-12-07\)](https://kunden.dwd.de/obf/(2022-12-07)).
- Emmerson, K.M., Carlslaw, N., Carlslaw, D., Lee, J.D., McFiggans, G., Bloss, W.J., Gravesock, T., Heard, D.E., Hopkins, J., Ingham, T., 2007. Free radical modelling studies during the UK TORCH Campaign in Summer 2003. *Atmos. Chem. Phys.* 7, 167–181. <https://doi.org/10.5194/acp-7-167-2007>.
- Epstein, Y., Moran, D.S., 2006. Thermal comfort and the heat stress indices. *Ind. Health* 44, 388–398. <https://doi.org/10.2486/indhealth.44.388>.
- Erhardt, D., Antretter, F., 2012. Applicability of regional model climate data for hygrothermal building simulation and climate change impact on the indoor environment of a generic church in Europe. In: *Proceedings of the 2nd European Workshop on Cultural Heritage Preservation EWCHP-2012*, Kjeller, Norway.
- EU, 2008. European Union Air Quality Standards Directive 2008/50/EC. European Union, Luxembourg. [https://environment.ec.europa.eu/topics/air/air-quality/eu-air-quality-standards\\_en](https://environment.ec.europa.eu/topics/air/air-quality/eu-air-quality-standards_en).
- Fanger, P.O., 1970. *Thermal Comfort. Analysis and Applications in Environmental Engineering*. Danish Technical Press, Copenhagen.
- Fischer, E.M., Schär, C., 2010. Consistent geographical patterns of changes in high-impact European heatwaves. *Nat. Geosci.* 3, 398–403. <https://doi.org/10.1038/ngeo866>.
- Fischer, P.H., Brunekreef, B., Lebert, E., 2004. Air pollution related deaths during the 2003 heat wave in The Netherlands. *Atmos. Environ.* 38, 1083–1085. <https://doi.org/10.1016/j.atmosenv.2003.11.010>.
- Fisk, W.J., 2015. Review of some effects of climate change on indoor environmental quality and health and associated no-regrets mitigation measures. *Build. Environ.* 86, 70–80. <https://doi.org/10.1016/j.buildenv.2014.12.024>.
- Fisk, W.J., Singer, B.C., Chan, W.R., 2020. Association of residential energy efficiency retrofits with indoor environmental quality, comfort, and health: a review of empirical data. *Build. Environ.* 180. <https://doi.org/10.1016/j.buildenv.2020.107067>.
- Fromme, H., Debiak, M., Sagunski, H., Röhl, C., Kraft, M., Kolossa-Gehring, M., 2019. The German approach to regulate indoor air contaminants. *Int. J. Hyg. Environ. Health* 222, 347–354. <https://doi.org/10.1016/j.ijheh.2018.12.012>.
- GEG, 2020. Building Energy Act (Gebäudeenergiegesetz). Federal Gazette, Berlin. <https://www.gesetze-im-internet.de/geg/GEG.pdf>.
- Geiss, O., Giannopoulos, G., Tirendi, S., Barrero-Moreno, J., Larsen, B.R., Kotzias, D., 2011. The AIRMEX study-VOC measurements in public buildings and schools/ kindergartens in eleven European cities: statistical analysis of the data. *Atmos. Environ.* 45, 3676–3684. <https://doi.org/10.1016/j.atmosenv.2011.04.037>.
- Giles, B.D., Balafoutis, C., Maheras, P., 1990. Too hot for comfort: the heatwaves in Greece in 1987 and 1988. *Int. J. Biometeorol.* 34, 98–104. <https://doi.org/10.1007/BF01093455>.
- Giorgi, F., Meleux, F., 2007. Modelling the regional effects of climate change on air quality. *C. R. Geosci.* 339, 721–733. <https://doi.org/10.1016/j.crte.2007.08.006>.
- Gutiérrez, J.M., Jones, R.G., Narisma, G.T., Alves, L.M., Amjad, M., Gorodetskaya, I.V., Grose, M., Klutse, N.A.B., Krakovska, S., Li, J., Martínez-Castro, D., Mearns, L.O., Mernild, S.H., Ngo-Duc, T., van den Hurk, B., Yoon, J.-H., 2021. Atlas. In: *Climate Change 2021: the Physical Science Basis. Contribution of Working Group I to the Sixth Assessment Report of the Intergovernmental Panel on Climate Change*. Cambridge University Press. <http://interactive-atlas.ipcc.ch/>.
- Hamdy, M., Carlucci, S., Hoes, P.-J., Hensen, J.L.M., 2017. The impact of climate change on the overheating risk in dwellings—a Dutch case study. *Build. Environ.* 122, 307–323. <https://doi.org/10.1016/j.buildenv.2017.06.031>.
- Hellén, H., Tykkä, T., Hakola, H., 2012. Importance of monoterpenes and isoprene in urban air in northern Europe. *Atmos. Environ.* 59, 59–66. <https://doi.org/10.1016/j.atmosenv.2012.04.049>.
- Holland, F., Aschmutat, U., Hesslering, M., Hofzumahaus, A., Ehhalt, D., 1998. Highly time resolved measurements of OH during POPCORN using laser-induced fluorescence spectroscopy. In: Rudolph R.K., J. (Ed.), *Atmospheric Measurements during POPCORN—Characterisation of the Photochemistry over a Rural Area*. Springer, Dordrecht.
- Holland, F., Hofzumahaus, A., Schäfer, J., Kraus, A., Pätz, H.W., 2003. Measurements of OH and HO2 radical concentrations and photolysis frequencies during BERLIOZ. *J. Geophys. Res. Atmos.* 108(D4), <https://doi.org/10.1029/2001JD001393>, 8246.
- Hukka, A., Viitanen, H.A., 1999. A mathematical model of mould growth on wooden material. *Wood Sci. Technol.* 33, 475–485. <https://doi.org/10.1007/s002260050131>.
- Intergovernmental Panel on Climate Change, 2021. *Climate Change 2021: the Physical Science Basis*. Cambridge. <https://www.ipcc.ch/report/ar6/wg1/>.
- ISO/DIS 7730, 2023. *Ergonomics of the Thermal Environment - Analytical Determination and Interpretation of Thermal Comfort Using Calculation of the PMV and PPD Indices and Local Thermal Comfort Criteria*. International Organization for Standardization, Geneva.
- Iturbide, M., Fernández, J., Gutiérrez, J.M., Bedia, J., Cimadevilla, E., Díez-Sierra, J., Manzanar, R., Casanueva, A., Baño-Medina, J., Milovac, J., Herrera, S., Cofiño, A.S., San Martín, D., García-Díez, M., Hauser, M., Huard, D., Yelekci, Ö., 2021. Repository Supporting the Implementation of FAIR Principles in the IPCC-WG1 Atlas. Zenodo. <https://github.com/IPCC-WG1/Atlas>.
- Jacob, D.J., Winner, D.A., 2009. Effect of climate change on air quality. *Atmos. Environ.* 43, 51–63. <https://doi.org/10.1016/j.atmosenv.2008.09.051>.
- Jenkin, M.E., Saunders, S.M., Pilling, M.J., 1997. The tropospheric degradation of volatile organic compounds: a protocol for mechanism development. *Atmos. Environ.* 31, 81–104. [https://doi.org/10.1016/S1352-2310\(96\)00105-7](https://doi.org/10.1016/S1352-2310(96)00105-7).
- Kahlenborn, W., Porst, L., Voß, M., Fritsch, U., Renner, K., Zebisch, M., Wolf, M., Schönthaler, K., Schauer, I., 2021. *Climate Impact and Risk Assessment 2021 for Germany (Summary)*. German Environment Agency, Dessau-Roßlau.
- Karlsson, P.E., Klingberg, J., Engardt, M., Andersson, C., Langner, J., Karlsson, G.P., Pleijel, H., 2017. Past, present and future concentrations of ground-level ozone and potential impacts on ecosystems and human health in northern Europe. *Sci. Total Environ.* 576, 22–35. <https://doi.org/10.1016/j.scitotenv.2016.10.061>.
- Krähenmann, S., Walter, A., Brien, S., Imbery, F., Matzarakis, A., 2016. Monthly, Daily and Hourly Grids of 12 Commonly Used Meteorological Variables for Germany Estimated by the Project TRY Advancement. DWD Climate Data Center.
- Lacressonnière, G., Watson, L., Gauss, M., Engardt, M., Andersson, C., Beekmann, M., Colette, A., Foret, G., Josse, B., Maréchal, V., Nyiri, A., Siour, G., Sobolowski, S., Vautard, R., 2017. Particulate matter air pollution in Europe in a +2 °C warming world. *Atmos. Environ.* 154, 129–140. <https://doi.org/10.1016/j.atmosenv.2017.01.037>.

- Langner, J., Engardt, M., Baklanov, A., Christensen, J., Gauss, M., Geels, C., Hedegaard, G.B., Nuterman, R., Simpson, D., Soares, J., 2012. A multi-model study of impacts of climate change on surface ozone in Europe. *Atmos. Chem. Phys.* 12, 10423–10440. <https://doi.org/10.5194/acp-12-10423-2012>.
- Lee, J.D., Lewis, A.C., Monks, P.S., Jacob, M., Hamilton, J.F., Hopkins, J.R., Watson, N. M., Saxton, J.E., Ennis, C., Carpenter, L.J., Carslaw, N., Fleming, Z., Bandy, B.J., Oram, D.E., Penkett, S.A., Slemr, J., Norton, E., Rickard, A.R., K Whalley, L., Heard, D.E., Bloss, W.J., Gravesstock, T., Smith, S.C., Stanton, J., Pilling, M.J., Jenkin, M.E., 2006. Ozone photochemistry and elevated isoprene during the UK heatwave of August 2003. *Atmos. Environ.* 40, 7598–7613. <https://doi.org/10.1016/j.atmosenv.2006.06.057>.
- Leissner, J., Kilian, R., Kotova, L., Jacob, D., Mikolajewicz, U., Broström, T., Ashley-Smith, J., Schellen, H.L., Martens, M., van Schijndel, J., 2015. Climate for Culture: assessing the impact of climate change on the future indoor climate in historic buildings using simulations. *Herit. Sci.* 3, 1–15. <https://doi.org/10.1186/s40494-015-0067-9>.
- Mansouri, A., Wei, W., Alessandrini, J.-M., Mandin, C., Blondeau, P., 2022. Impact of climate change on indoor air quality: a review. *Int. J. Environ. Res. Publ. Health* 19, 15616. <https://doi.org/10.3390/ijerph192315616>.
- McArdle, W.D., Katch, F.I., Katch, V.L., 2014. *Exercise Physiology: Nutrition, Energy, and Human Performance*. Wolters Kluwer, Baltimore, MD.
- Meleux, F., Solmon, F., Giorgi, F., 2007. Increase in summer European ozone amounts due to climate change. *Atmos. Environ.* 41, 7577–7587. <https://doi.org/10.1016/j.atmosenv.2007.05.048>.
- Melkonyan, A., Kuttler, W., 2012. Long-term analysis of NO, NO<sub>2</sub> and O<sub>3</sub> concentrations in North Rhine-Westphalia, Germany. *Atmos. Environ.* 60, 316–326. <https://doi.org/10.1016/j.atmosenv.2012.06.048>.
- Melkonyan, A., Wagner, P., 2013. Ozone and its projection in regard to climate change. *Atmos. Environ.* 67, 287–295. <https://doi.org/10.1016/j.atmosenv.2012.10.023>.
- Nazaroff, W.W., 2013. Exploring the consequences of climate change for indoor air quality. *Environ. Res. Lett.* 8, 015022. <https://doi.org/10.1088/1748-9326/8/1/015022>.
- Nazaroff, W.W., 2016. Indoor bioaerosol dynamics. *Indoor Air* 26, 61–78. <https://doi.org/10.1111/ina.12174>.
- Nazaroff, W.W., 2022. Indoor aerosol science aspects of SARS-CoV-2 transmission. *Indoor Air* 32, e12970. <https://doi.org/10.1111/ina.12970>.
- Nazaroff, W.W., Weschler, C.J., 2022. Indoor ozone: concentrations and influencing factors. *Indoor Air* 32, e12942. <https://doi.org/10.1111/ina.12942>.
- Nevalainen, A., Täubel, M., Hyvärinen, A., 2015. Indoor fungi: companions and contaminants. *Indoor Air* 25, 125–156. <https://doi.org/10.1111/ina.12182>.
- Nussbaumer, C.M., Crowley, J.N., Schuladen, J., Williams, J., Hafermann, S., Reiff, A., Axinte, R., Harder, H., Ernest, C., Novelli, A., 2021. Measurement report: photochemical production and loss rates of formaldehyde and ozone across Europe. *Atmos. Chem. Phys.* 21, 18413–18432. <https://doi.org/10.5194/acp-21-18413-2021>.
- Pu, X., Wang, T., Huang, X., Melas, D., Zanis, P., Papanastasiou, D., Poupkou, A., 2017. Enhanced surface ozone during the heat wave of 2013 in Yangtze River Delta region, China. *Sci. Total Environ.* 603, 807–816. <https://doi.org/10.1016/j.scitotenv.2017.03.056>.
- Rohrer, F., Berresheim, H., 2006. Strong correlation between levels of tropospheric hydroxyl radicals and solar ultraviolet radiation. *Nature* 442, 184–187. <https://doi.org/10.1038/nature04924>.
- Sacht, H., Bragança, L., Almeida, M., Nascimento, J.H., Caram, R., 2016. Spectrophotometric characterization of simple glazings for a modular façade. *Energy Proc.* 96, 965–972. <https://doi.org/10.1016/j.egypro.2016.09.175>.
- Salthammer, T., Morrison, G.C., 2022. Temperature and indoor environments. *Indoor Air* 32, e13022. <https://doi.org/10.1111/ina.13022>.
- Salthammer, T., Schieweck, A., Gu, J., Ameri, S., Uhde, E., 2018. Future trends in ambient air pollution and climate in Germany – implications for the indoor environment. *Build. Environ.* 143, 661–670. <https://doi.org/10.1016/j.buildenv.2018.07.050>.
- Salthammer, T., Zhao, J., Schieweck, A., Uhde, E., Hussein, T., Antretter, F., Künzel, H., Pazold, M., Radon, J., Birmili, W., 2022. A holistic modeling framework for estimating the influence of climate change on indoor air quality. *Indoor Air* 32, e13039. <https://doi.org/10.1111/ina.13039>.
- Sarwar, G., Corsi, R., Kimura, Y., Allen, D., Weschler, C.J., 2002. Hydroxyl radicals in indoor environments. *Atmos. Environ.* 36, 3973–3988. [https://doi.org/10.1016/S1352-2310\(02\)00278-9](https://doi.org/10.1016/S1352-2310(02)00278-9).
- Schär, C., Jendritzky, G., 2004. Hot news from summer 2003. *Nature* 432, 559–560. <https://doi.org/10.1038/432559a>.
- Schieweck, A., Uhde, E., Salthammer, T., Salthammer, L.C., Morawska, L., Mazaheri, M., Kumar, P., 2018. Smart homes and the control of indoor air quality. *Renew. Sustain. Energy Rev.* 94, 705–718. <https://doi.org/10.1016/j.rser.2018.05.057>.
- Shaw, D., Carslaw, N., 2021. INCHEM-Py: an open source Python box model for indoor air chemistry. *J. Open Source Softw.* 6, 3224. <https://doi.org/10.21105/joss.03224>.
- Shaw, D.R., Carter, T.J., Davies, H.L., Harding-Smith, E., Crocker, E.C., Beel, G., Wang, Z., Carslaw, N., 2023. INCHEM-Py v1.2: A Community Box Model for Indoor Air Chemistry, vol. 2023. *EGUsphere* [preprint], pp. 1–32. <https://doi.org/10.5194/egusphere-2023-1328>.
- Steuil, K., Schade, M., Heudorf, U., 2018. Mortality during heatwaves 2003–2015 in Frankfurt-Main – the 2003 heatwave and its implications. *Int. J. Hyg. Environ. Health* 221, 81–86. <https://doi.org/10.1016/j.ijheh.2017.10.005>.
- Terry, A.C., Carslaw, N., Ashmore, M., Dimitroulopoulou, S., Carslaw, D.C., 2014. Occupant exposure to indoor air pollutants in modern European offices: an integrated modelling approach. *Atmos. Environ.* 82, 9–16. <https://doi.org/10.1016/j.atmosenv.2013.09.042>.
- Vardoulakis, S., Dimitroulopoulou, C., Thornes, J., Lai, K.-M., Taylor, J., Myers, I., Heaviside, C., Mavrogianni, A., Shrubsole, C., Chalabi, Z., Davies, M., Wilkinson, P., 2015. Impact of climate change on the domestic indoor environment and associated health risks in the UK. *Environ. Int.* 85, 299–313. <https://doi.org/10.1016/j.envint.2015.09.010>.
- Vautard, R., Honore, C., Beekmann, M., Rouil, L., 2005. Simulation of ozone during the August 2003 heat wave and emission control scenarios. *Atmos. Environ.* 39, 2957–2967. <https://doi.org/10.1016/j.atmosenv.2005.01.039>.
- Vieno, M., Dore, A., Stevenson, D.S., Doherty, R., Heal, M.R., Reis, S., Hallsworth, S., Tarrason, L., Wind, P., Fowler, D., 2010. Modelling surface ozone during the 2003 heat-wave in the UK. *Atmos. Chem. Phys.* 10, 7963–7978. <https://doi.org/10.5194/acp-10-7963-2010>.
- Viitanen, H., Krus, M., Ojanen, T., Eitner, V., Zirkelbach, D., 2015. Mold risk classification based on comparative evaluation of two established growth models. *Energy Proc.* 78, 1425–1430. <https://doi.org/10.1016/j.egypro.2015.11.165>.
- Wainman, T., Weschler, C.J., Lioy, P.J., Zhang, J., 2001. Effects of surface type and relative humidity on the production and concentration of nitrous acid in a model indoor environment. *Environ. Sci. Technol.* 35, 2200–2206. <https://doi.org/10.1021/es000879i>.
- Wang, Z., Shaw, D., Kahan, T., Schoemaeker, C., Carslaw, N., 2022. A modeling study of the impact of photolysis on indoor air quality. *Indoor Air* 32, e13054. <https://doi.org/10.1111/ina.13054>.
- Watson, L., Lacrosonnière, G., Gauss, M., Engardt, M., Andersson, C., Josse, B., Maréchal, V., Nyiri, A., Sobolowski, S., Siour, G., Szopa, S., Vautard, R., 2016. Impact of emissions and +2 °C climate change upon future ozone and nitrogen dioxide over Europe. *Atmos. Environ.* 142, 271–285. <https://doi.org/10.1016/j.atmosenv.2016.07.051>.
- Weller, B., Unnewehr, S., Tasche, S., Härth, K., 2009. *Glass in Building: Principles, Applications, Examples*. DETAIL-Institut für internationale Architektur-Dokumentation GmbH & Co. KG.
- Winkler, M., Antretter, F., Radon, J., 2017. Critical discussion of a shading calculation method for low energy building and passive house design. *Energy Proc.* 132, 33–38. <https://doi.org/10.1016/j.egypro.2017.09.627>.
- World Health Organization, 2009. WHO Guidelines for Indoor Air Quality: Dampness and Mould. World Health Organization, Regional Office for Europe, Copenhagen. <https://www.who.int/publications/i/item/9789289041683>.
- World Health Organization, 2021a. Heat and Health in the WHO European Region: Updated Evidence for Effective Prevention. World Health Organization, Regional Office for Europe, Copenhagen. <https://www.who.int/europe/publications/i/item/9789289055406>.
- World Health Organization, 2021b. WHO Global Air Quality Guidelines: Particulate Matter (PM<sub>2.5</sub> and PM<sub>10</sub>), Ozone, Nitrogen Dioxide, Sulfur Dioxide and Carbon Monoxide. World Health Organization, Geneva. <https://iris.who.int/handle/10665/345334>.
- Zhao, J., Birmili, W., Wehner, B., Daniels, A., Weinhold, K., Wang, L., Merkel, M., Kecorius, S., Tuch, T., Franck, U., 2020. Particle mass concentrations and number size distributions in 40 homes in Germany: indoor-to-outdoor relationships, diurnal and seasonal variation. *Aerosol Air Qual. Res.* 20, 576–589. <https://doi.org/10.4209/aaqr.2019.09.0444>.
- Zhong, L., Lee, C.S., Haghghat, F., 2017. Indoor ozone and climate change. *Sustain. Cities Soc.* 28, 466–472. <https://doi.org/10.1016/j.scs.2016.08.020>.